RSC Advances

ROYAL SOCIETY OF CHEMISTRY

www.rsc.org/advances

Graphical abstract

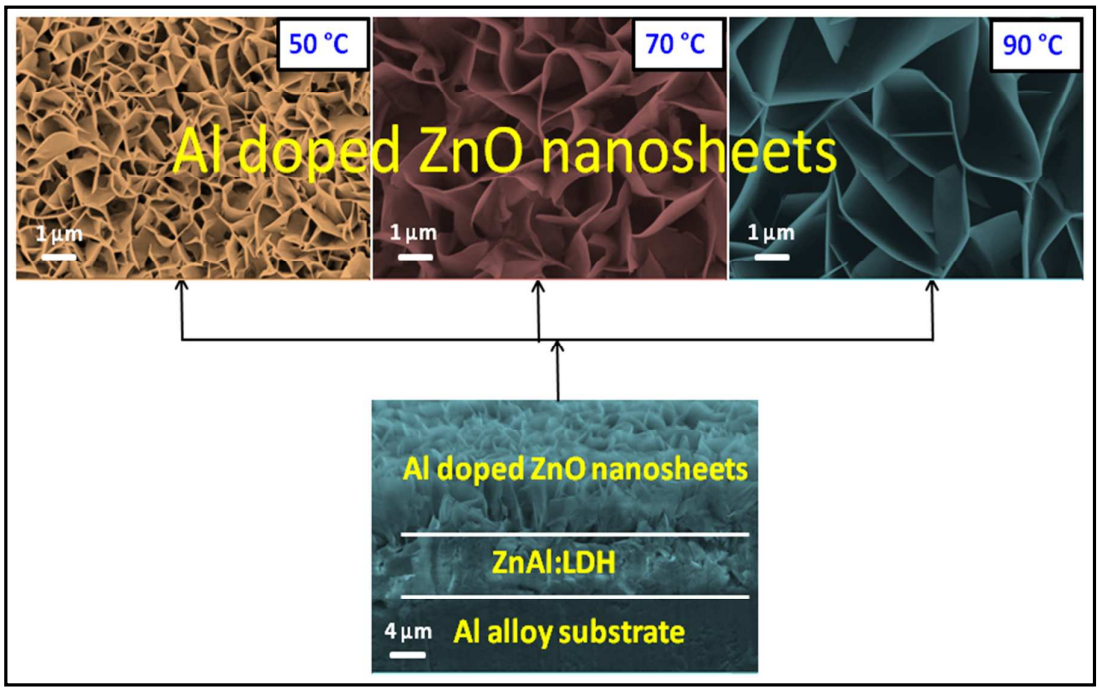

Morphology controlled synthesis of Al doped ZnO nanosheets on Al alloy substrate by low-temperature solution growth method

Venkateswarlu Gaddam[1,*], R. Rakesh Kumar[1,2], Mitesh Parmar[1], G R Krishna Yaddanapudi[3], M.M.Nayak[4] and K.Rajanna[1]

[1] Department of Instrumentation and Applied Physics, Indian Institute of Science, Bangalore 560012, India.

[2] Department of Physics, Gitam Univeristy Hyderabad campus, Hyderbad-502329.

[3] Department of Materials Engineering, Indian Institute of Science, Bangalore 560012, India.

[4] Centre for Nanoscience and Engineering, Indian Institute of Science, Bangalore 560012, India.

Abstract

We report, the morphology-controlled synthesis of aluminium (Al) doped Zinc oxide (ZnO) nanosheets on Al alloy (AA-6061) substrate by low-temperature-solution growth method without using any external seed layer and doping process. Doped ZnO nanosheets were obtained at low temperatures of 60-90 °C for the growth time of 4 hours. In addition to the synthesis, the effect of growth temperature on the morphological changes of ZnO nanosheets is also reported. As-synthesized nanosheets are characterized by FE-SEM, XRD TEM and XPS for their morphology, crystallinity, microstructure and compositional analysis respectively. The doping of Al in ZnO nanosheets is confirmed with EDXS and XPS. Further, effect of growth temperature on the morphological changes was studied in the range of 50 to 95 °C. It was found that the thickness and height of nanosheets varied with respect to the growth temperature. The study has given an important insight of the structural morphology with respect to the growth temperature, which in turn enabled to determine growth temperature window for the ZnO nanosheets. These Al doped ZnO nanosheets have

the potential application possibilities in gas sensors, solar cells and energy harvesting devices like nanogenerators.

Key words: ZnO, Nanosheets, Al alloy substrate, Low-temperature growth, Doping, Growth temperature window.

*** Corresponding author**

E-mail: kraj@isu.iisc.ernet.in

Tel: +91-80-2293 3188, Fax: +91-80-2360 0135

1. Introduction

One dimensional (1D) Zinc Oxide (ZnO) nanostructures have attracted much attention during the last couple of decades due to their excellent optical, electrical, semiconducting and piezoelectric properties. These features enabled for their wide applicability in many fields including electronics, optoelectronics, electromechanical and electrochemical [1-8]. However, recently two dimensional (2D) ZnO nanostructures, namely nanowalls [9-10], nanoplatelets [11, 12] and nanosheets [13-22], are becoming more popular due to their properties like nanometer-scale thickness, high surface to volume ratio and good mechanical stability [14,18-20]. In this context, the 2D ZnO nanostructures are widely used in UV detectors [16], gas sensors [23], energy conversion and storage devices [24], field emission devices [25], solar cells [26], superhydrophilicity and photocatalytic properties [23,12] and nanogenerators [14-15]. On the performance enhancement characteristics of 2D ZnO nanostructures, several reports have been published [13, 23]. One of the ways to vary the material properties is by the process of doping these nanostructures with suitable external materials. As a result, these dopants create defects and impurities, which can play significant role in optical as well as electrical properties and hence affect the overall performance characteristics of nanostructure systems [13, 23]. The various materials used as dopants for ZnO nanostructures are B, Al, Ga, In, etc. [27]. In case of Al doping, the doped ZnO nanostructures can improve the film conductivity, photocatalytic activity, electronic transport enhancement, especially in gas sensors [13, 23]. In general, the Al doping process for the ZnO nanostructures can be performed by altering the synthesis process or using an external precursors of Al. However, direct fabrication of Al doped ZnO nanosheets with single step synthesis process is still challenging and noteworthy.

Generally, the ZnO nanosheets are synthesized by various methods such as solvothermal method [13], microwave assisted synthesis [16], thermal evaporation [19],

hydrothermal synthesis method [14, 17-18, 20], carbothermal reduction process [21] and electrodepostion [28]. Among them, solution growth assisted hydrothermal method is the most favourable for the growth of Al doped 2D nanostructures due to its flexibility to carry out the synthesis process on variety of substrates at low temperatures, uniform growth at large area surfaces, relatively simple, cost effective, less hazardous and environmental friendly [18,20].

Various studies have been reported in the literature on the growth of ZnO nanosheets on variety of substrates like glass [13], polyether sulphone (PES)[14], polyethylene terephthalate (PET) [15], Al [17] and Si [29]. It is important to note that, in majority of the cases external seed layer has been employed. To the best of our knowledge, there is no report on the use of Al alloy substrate (AA-6061), for the growth of ZnO nanosheets by low-temperature solution growth method.

Herein, we report on the growth of Al doped ZnO nanosheets on Al alloy substrate without the use of any external seed layer as well as Al precursors at <100 °C by solution growth method. This Al alloy substrate facilitates the growth of nanosheets and also it acts as a source for Al doping during the nanosheets growth process. Subsequently, it can also serves as a better bottom electrode for device applications. In addition to the above, we are also reporting the effect of growth temperature for the synthesis of ZnO nanosheets on Al alloy substrate. It is important to know the effect of growth temperature because it will be helpful in deciding the ideal optimum growth temperature for ZnO nanosheets and minimize the power consumption during the synthesis. Moreover, it will also be useful to understand the 2D nanosheet structure's mechanical, optical and electrical properties. This in turn enables to choose the better properties of nanosheets for device applications.

2. Experimental

2.1 Synthesis of 2D ZnO nanosheets

Prior to synthesis of ZnO nanosheets, Al alloy substrate was thoroughly cleaned using acetone, isopropyl alcohol and subsequently with DI (de-ionized) water by ultrasonication for 10 minutes. Cleaned alloy substrate was directly used for the growth of ZnO nanosheets without depositing any additional seed layer. The nanosheets were grown by using a simple hydrothermal method. In this process, an aqueous solution consisting of an equal amount of zinc nitrate hexahydrate (Zn $(NO_3)_2.6H_2O$) and hexamethyletetramine (HMTA, $C_6H_{12}N_4$) with the concentration of 25 mM was prepared. The substrate was placed over the surface of solution (60 ml) in a screw reagent bottle. Further, it was maintained at different growth temperatures ranging from 60-90 °C in steps of 10 °C for 4 hours duration by keeping the bottle inside the hot air oven (See S1 supplementary information). After the growth process, the substrate was allowed to cool down to room temperature. Subsequently, the substrate was taken out and thoroughly cleaned with DI water for removing the organic salts and it was allowed to dry at room temperature [2, 14, 17, 20]. After this process, the formation of white coloured nanostructured film was observed over the substrate.

2.2 Characterization

As-synthesized nanostructured ZnO films on Al alloy substrate were characterized by the following measurement techniques.

X-ray diffraction (XRD) studies were carried out by Bruker D8 Advance diffractometer (Model no: A18-A100/ D76182 Karl sruhe, Germany) in reflective mode powered at 40 kV and 30 mA at room temperature. The crystalline phase of the films were examined using Cu Kα radiation (λ = 1.5406 Å) with nickel filter at a scan rate of 2° min^{-1}.

Field-emission scanning electron microscopy (FE-SEM) measurements were carried out by Carl Zeiss, Ultra 55 instrument equipped with SE2 and InLense detectors. Microscopic images were acquired with an accelerating voltage between 5-10 kV. Energy dispersive X-ray spectroscopy (EDXS) measurements were carried out with the same instrument equipped with an Oxford INCA x-sight X-ray detector. The EDXS data was acquired at an accelerating voltage of 15 kV.

Transmission electron microscopy (TEM) and high resolution (HR-TEM) analyses were carried out using a TEM, T20, Tecnai20 D2060 U-Twin microscope operated at 200 kV and having a 0.19 nm point resolution. The sample was prepared specially by scraping the portion of nanosheet film from the substrate and dispersed it in acetone solution for the purpose of examining the same using TEM. The solution prepared was subjected to ultrasonication for 5 min. Finally, the solution was drop casted onto a carbon coated copper grid and dried.

X-ray photoelectron spectroscopy (XPS, Kratos Axis Ultra DLD system) spectra were recorded using Al Kα radiation dual anode source (Energy, hυ = 1486.6 eV) with X-Ray power 150W in ultra high vacuum environment at a base pressure of 3 x 10^{-9} Torr. All peaks were calibrated with respect to carbon (C 1s) at 284.8 eV. The XPS analysis was carried out at constant pass energy of 160 eV for survey scans and 20 eV for high-resolution scans. The data fitting and quantification analysis were carried out using CASA XPS software after considering relative sensitivity factors (RSF) for each element of the compound. Gaussian–Lorenzian functions and Shirley type background were employed during the analysis. Depth profile measurements were carried out with Ar^+ ion gas at gun voltage 4kV.

3. Results and discussion

The surface morphologies of as-grown nanostructures on Al alloy substrate maintained at different growth temperatures of 90-60 °C are shown in Figures 1 (a)-(d) respectively. As can be seen, in all the cases, porous network of ZnO nanosheets are present all over the Al alloy substrate and are randomly distributed. Along with their randomness, the non-uniform interconnections are certainly seen in the electron microscopy images (Figure 1(a)-(d)). The cross-sectional analysis of the nanosheets network is analyzed and shown in Figure 2 (a)-(d). As can be observed in these images, all the nanosheets grown are relatively vertical to the substrate. The nanosheets grown at 90°C are having flat surface and the average height and thickness of each sheet are ~6.5±0.04 μm and ~84.15±2.9 nm respectively. However, at lower growth temperatures of 80 °C, 70 °C and 60 °C, the surface of each nanosheet is more curved and the curvature increased drastically with the increase of growth temperature (Figures 1(a-d)). The average height of each nanosheet is about 3.03±0.10 μm, 2.39±0.02 μm and 2.19±0.09 μm & the thickness of each sheet is about 41.99±2.3 nm, 33.75±1.6 nm and 22.91±1.3 nm, respectively.

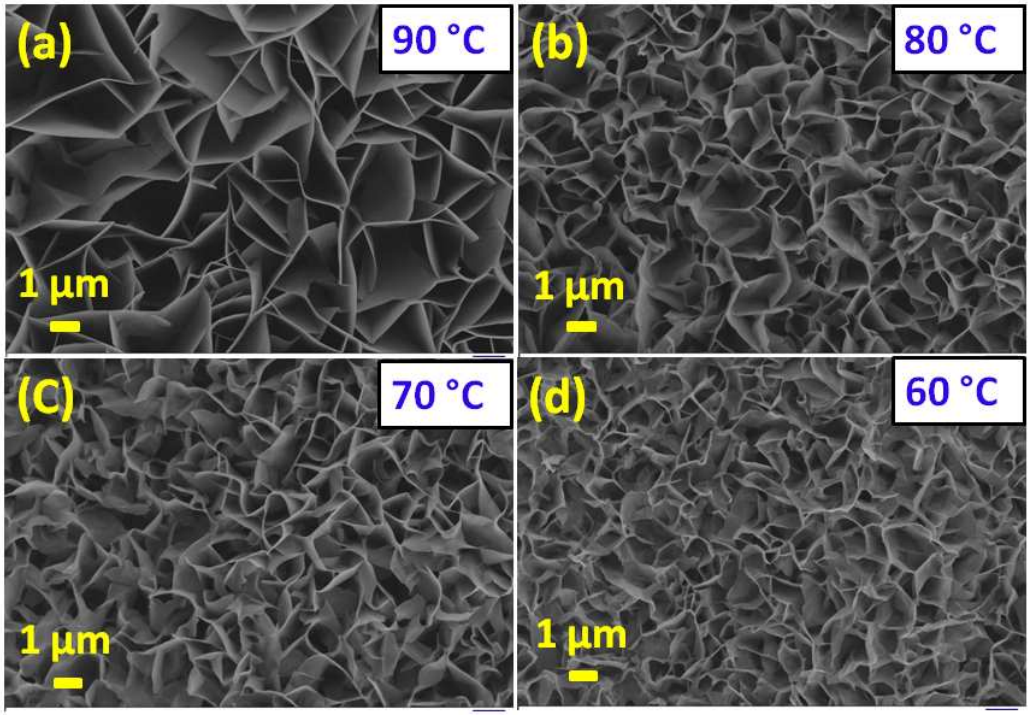

Figure 1: Top view of FE-SEM images for ZnO nanosheets synthesized at different growth temperatures of (a) 90 °C, (b) 80 °C, (c) 70 °C, (d) 60 °C.

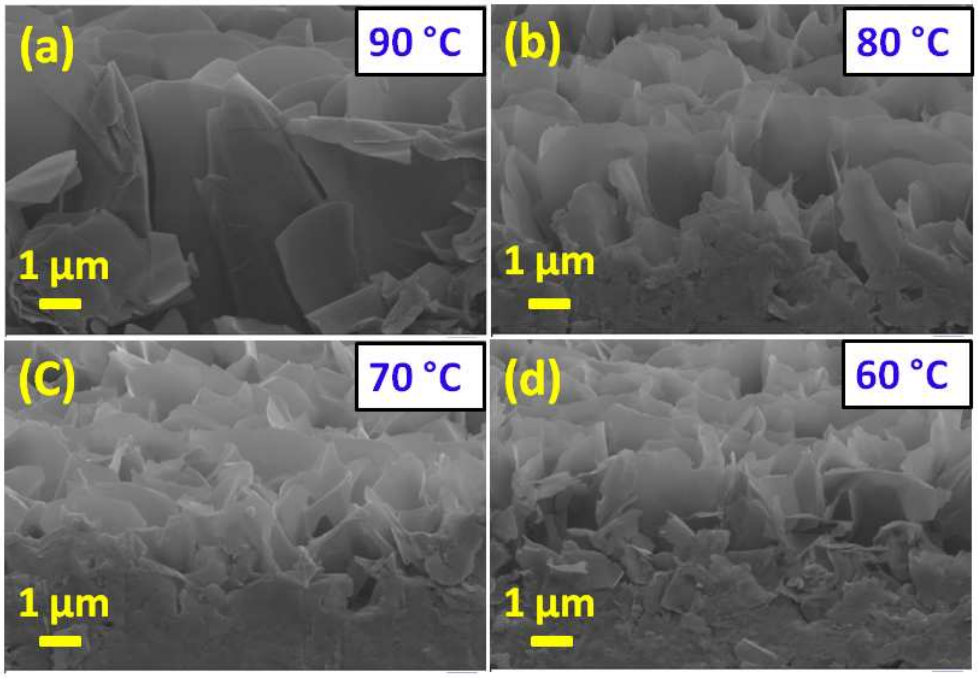

Figure 2: Cross-sectional view of FE-SEM images for ZnO nanosheets synthesis at different growth temperatures of (a) 90 °C, (b) 80 °C, (c) 70 °C, (d) 60 °C.

Graphical representation of the variation of average height and thickness with growth temperature are shown in Figure 3 (a-b) (see *Table1* supplementary information). It is clearly evident that the growth temperature has a pronounced effect on the morphology in terms of thickness as well as height of each nanosheet. In the growth temperature range between 90°C and 60 °C, the height and thickness of nanosheets decreased to about 3-4 times. This temperature dependent thickness variation behaviour of the nanosheets is similar to the observation reported by Cheng *et al.*[18] It is true in the present study even at the growth temperatures of less than 100 °C.

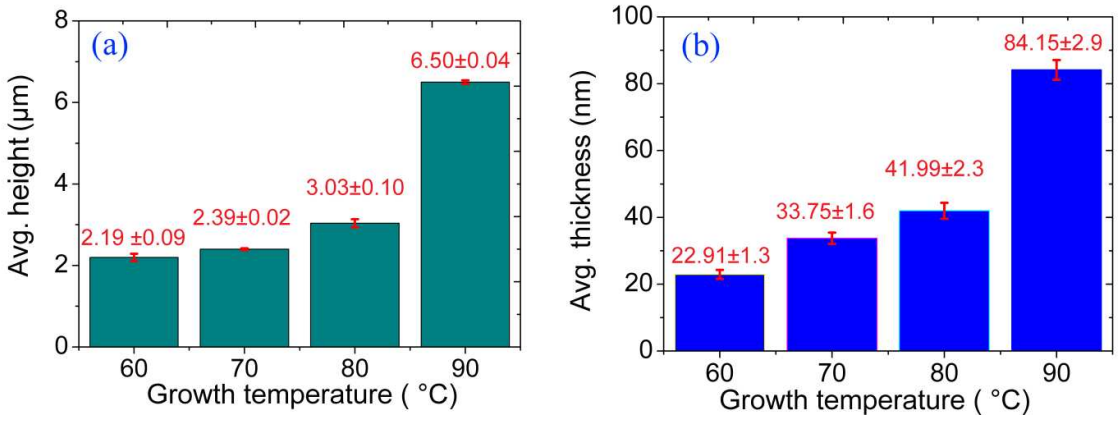

Figure 3: Effect of growth temperature variations on height and thickness of ZnO nanosheets.

We have studied the effect of growth temperature even at 95 °C and found that the thickness and height of the nanosheets increased much more (see S2 supplementary information). Further, nanosheets growth study was performed at lower growth temperature of < 60 °C. Interestingly, at the growth temperature of 50 °C nanosheets growth was confined to only on few selected areas of the substrate (see S3 supplementary information).

Furthermore, the nanosheets growth study was performed at 40 °C and found that there was no growth of nanosheets network due to insufficient thermal energy (see S4 supplementary information). Therefore, it is concluded that the nanosheets growth starts from the growth temperature of 50 °C onwards.

Further, energy dispersive X-ray analysis spectroscopy (EDXS) spectrum recorded on the surface of the 2D ZnO nanosheets showed the presence of Zn, Al and O (see S5 (a-b) supplementary information). The presence of Al element could be from the substrate or from the nanosheets. In order to confirm the fact that whether Al signal is coming from the substrate or the ZnO nanosheets, the EDXS study was performed confining only on cross sectional region of ZnO nanosheets as indicated in Figure S5 (see S5 (c-d) supplementary information) as well on the single ZnO nanosheet (Figure 4). Surprisingly, Al content was found in the spectrum and hence confirmed the presence of Al in ZnO nanosheets. There was no Al precipitate nor Al particle on the single ZnO nanosheet, which confirms the fact that the ZnO nanosheets are doped with Al. The doping of Al is believed to be due to diffusion of Al from the substrate during the growth process. It is important to note that in our present work, without following any separate additional process step, we have succeeded in synthesizing Al doped ZnO nanosheets. The Al doping was further confirmed using different compositional analysis techniques such as TEM-EDS and XPS.

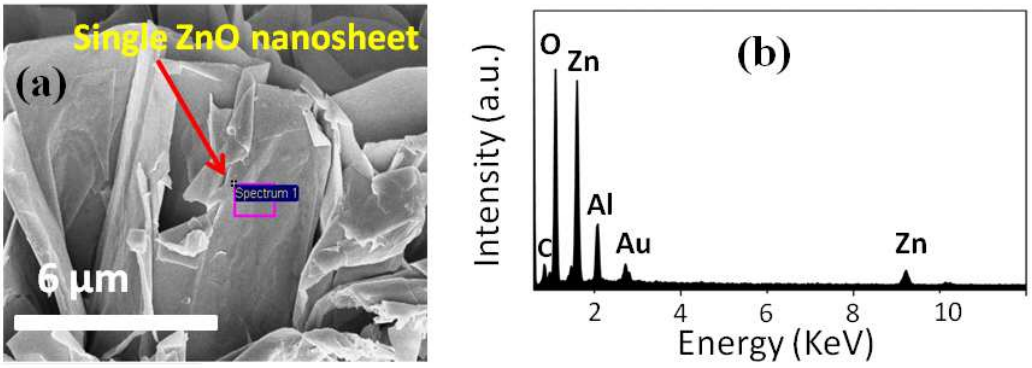

Figure 4: (a) FE-SEM image of single ZnO nanosheet (grown at 90 °C) from cross sectional view (b) Corresponding EDS spectrum.

X-ray diffraction (XRD) pattern of the ZnO nanosheets grown at different growth temperatures of 90 °C, 80 °C, 70 °C and 60 °C are recorded and shown in Figures 5 (a-d) respectively. The diffraction peak at 2θ=34.26° is corresponding to the (002) plane of the ZnO and confirms the formation of ZnO phase (JCPDF card # 36-1451). The XRD pattern with 2θ values in the range 33 to 35 for 2D ZnO nanosheets can be clearly seen in Figure 6 (a-d). The highly intense diffraction peaks at 2θ=38.29, 44.54 and 64.90 corresponds to (111), (200) and (220) planes of the bare Al alloy substrate (JCPDF card # 85-1327) (See S6 supplementary information).

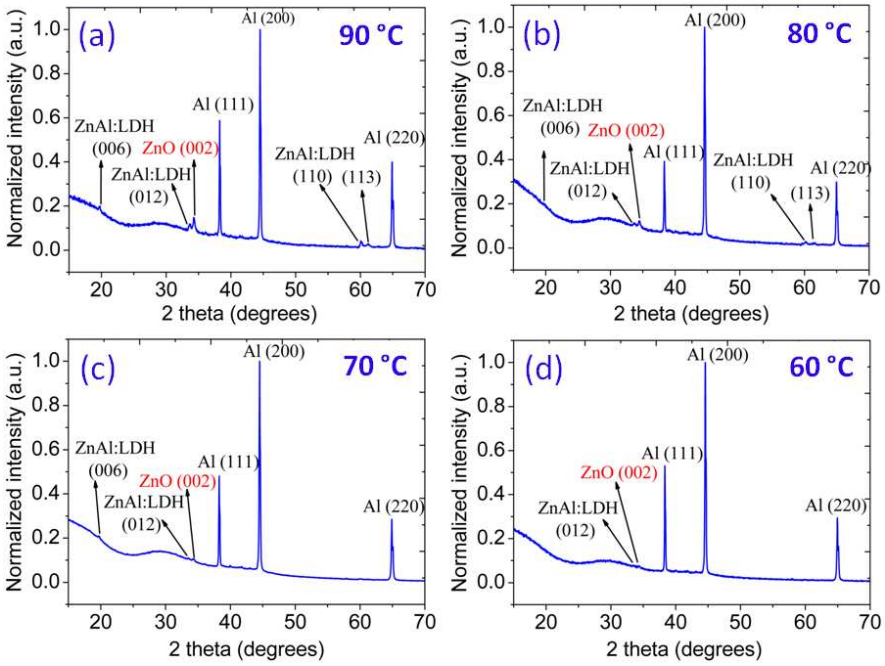

Figure 5: XRD pattern of 2D ZnO nanosheets on Al alloy substrate at different growth temperatures of (a) 90 °C, (b) 80 °C, (c) 70 °C, (d) 60 °C.

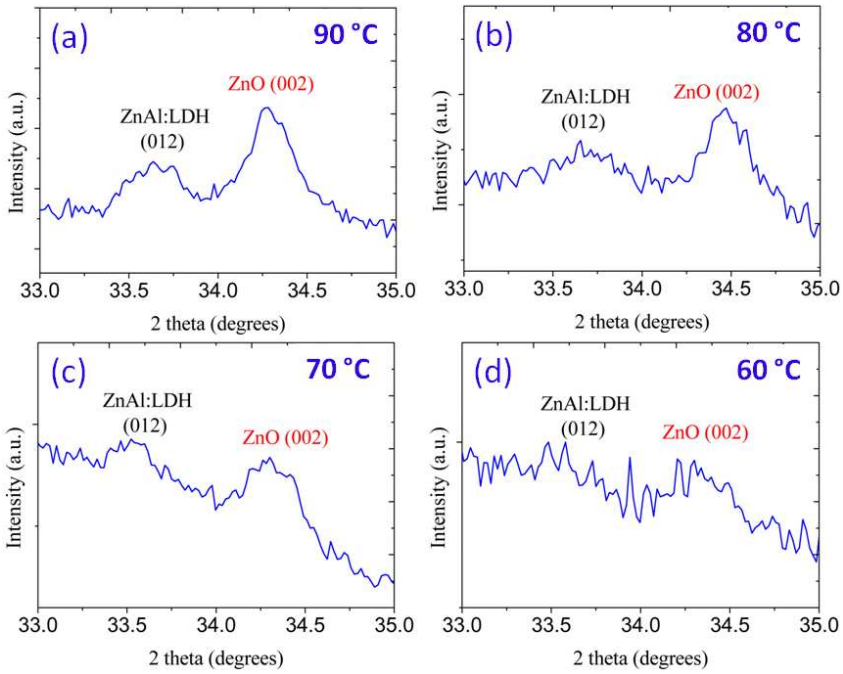

Figure 6: XRD pattern with 2 theta values from 33 to 35 of 2D ZnO nanosheets on Al alloy substrate at different growth temperatures of (a) 90 °C, (b) 80 °C, (c) 70 °C, (d) 60 °C.

The crystalline nature of ZnO nanosheets grown at 90 °C is having highest peak intensity as compared to other growth temperatures. The crystallinity of nanosheets grown at 95 °C is almost similar to the nanosheets grown at 90 °C (See S2 supplementary information). It was observed that the intensity of diffraction peaks decreased with the gradual reduction in growth temperature from 90 °C to 60 °C. This suggests the poor crystallization of ZnO at lower growth temperatures.

In addition to the ZnO Phase, the presence of ZnAl: LDH phase has also been observed which is similar to the observation reported by Kim *et al.* [14] This additional phase is evident from the XRD peaks (see in Figure 5) at 2θ=19.77°, 33.63° & 60.08° and the corresponding planes are (006), (012) & (110) of ZnAl:LDH [14, 30]. The LDH layer is also confirmed by the cross sectional FE-SEM image of the nanosheets on Al substrate (see S7

supplementary information). The cross sectional image clearly shows that the LDH layer was formed at the interface of ZnO nanosheets and Al alloy substrate [14].

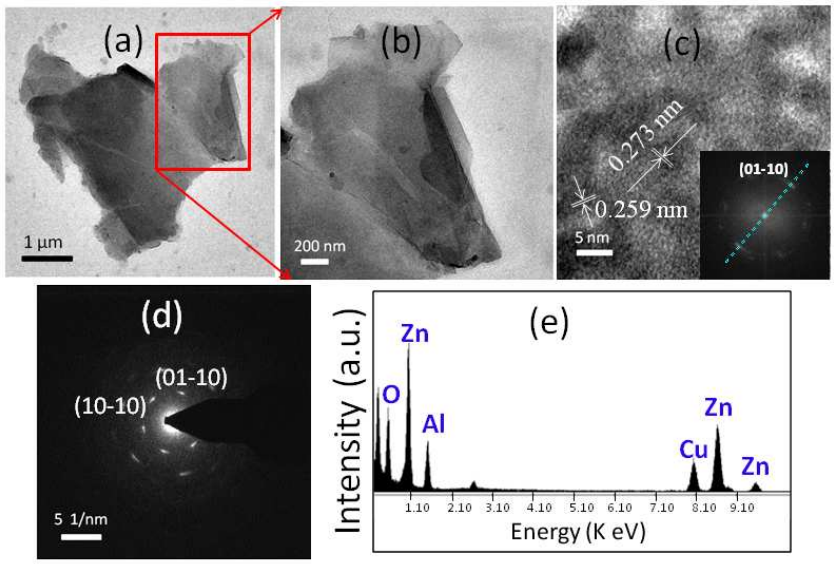

Figure 7: TEM images of ZnO nanosheets grown at 90 °C (a) Low magnification image, (b) High magnification image, (c) HR image (FFT image of the corresponding HR image in the inset), (d) SAED pattern and (e) EDS of corresponding TEM image.

Apart from the above, structural characterization and composition analysis of single ZnO nanosheet was carried out using TEM. Low and high magnification images of single nanosheet are shown in Figures 7 (a)-(b) respectively, which confirms the 2D nature of the nanosheet. The HR-TEM (High Resolution- TEM) image recorded on the single ZnO nanosheet is shown in Figure 7 (c) and it indicates the polycrystalline nature of 2D ZnO nanosheets [10, 17]. The measured d-spacing value from HR-TEM image and its FFT image (local diffraction) (inset Figure 7 (c)) is found to be 0.273 nm, which corresponds to interplanar spacing of (01-10) planes in ZnO. Figure 7 (d) shows the selected area electron diffraction (SAED) pattern recorded on same ZnO nanosheet and also reveals the polycrystalline nature of the sheet. It was observed that ZnO nanosheets were getting

damaged due to electron beam irradiation during TEM analysis. This kind of behaviour is similar to the observation reported in literature [17, 18]. This irradiation (before and after the radiation) damage by electron beam affected the crystallinity of the nanosheets (see S8 supplementary information). The EDXS measurement recorded on the single ZnO nanosheet is shown in Figure 7(e) wherein the presence of Zn, Al and O elements are clearly evident. The presence of Al reveals that the ZnO nanosheets grown are doped with Al element. The presence of Cu element is due to the carbon-coated TEM grid used for TEM analysis.

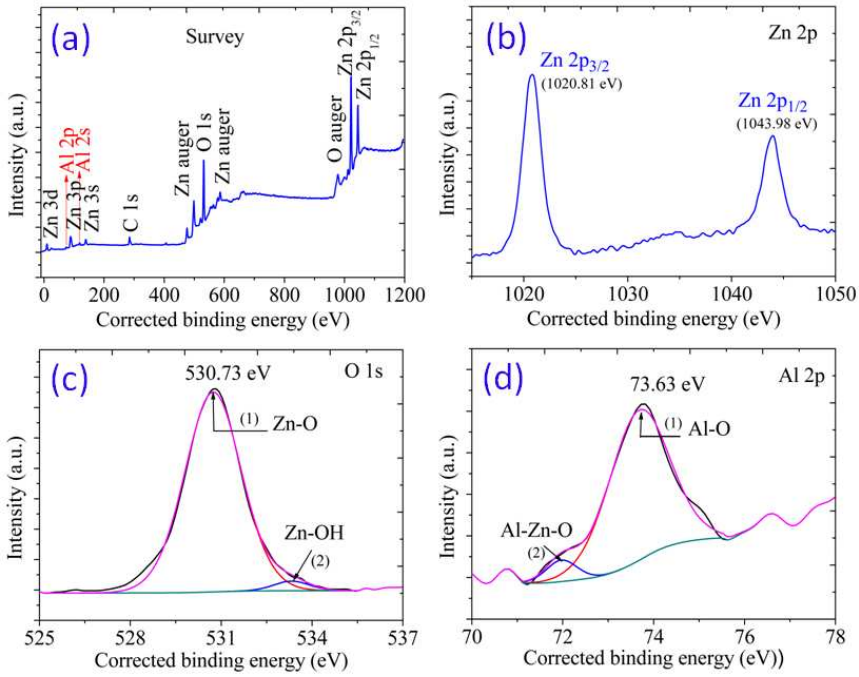

Figure 8: (a) XPS survey spectra, (b) Zn 2p peak, (c) O 1s peak and (d) Al 2p peak.

In order to find out the distribution and oxidation state of Al in ZnO nanosheets, the sample (grown at 90 °C) was subjected to surface analysis by XPS. The XPS survey spectra of the ZnO nanosheets are shown in Figure 8 (a). Only Zn, O, C and Al related core levels are observed in the survey spectrum. The C signal may originate from adventitious carbon contamination. The detailed quantification data of ZnO nanosheets is provided in the supplementary information (*Table 2*). The binding energies of Zn 2p core-level ZnO nanosheets have two fitting peaks located at about 1020.81 eV and 1043.98 eV, which are

attributed to Zn $2p_{3/2}$ and Zn $2p_{1/2}$ respectively as shown in figure 8 (b). These results indicate that the oxidation state of Zn at the surface of ZnO nanosheets is +2 [31]. In addition to that, the Auger parameter of Zn value (2009.09 eV) is in close agreement with the previously reported ZnO nanostructures, which confirms the formation of ZnO [11, 32]. Figure 8 (c) indicates the O 1s peaks centered at 530.73 eV and 533.33 eV and marked as peak-1 and peak-2, which were used to fit the experimental data. Peak-1, positioned at the lower binding energy of 530.73 eV, and is assigned to O^{2-} ions in the Zn–O bonding of the wurtzite structure of ZnO [28, 32]. The other peak-2 located at 533.33 eV is related to OH^- group absorbed onto the surface of the ZnO nanosheets. The existence of OH^- group in the nanosheets is due to the samples being prepared in solution method [28].

The observed Al-O binding energy peak at 73.63 eV (figure 8 (d)) can be attributed to the binding energy of Al 2p core level doublet. This binding energy is very close to the one in the literature (Al 2p: 73.9 eV) with oxidation state close to +3 [33] as well as lower than the pure Al_2O_3 (Al 2p: 75.6 eV) and above metallic Al (Al 2p: 72.8 eV) [34]. The exact bonding state of the peak at 71.97 eV is not understood well. Yet, it has been reported that the reduction in binding energy of Ga 3d peak in GaN grown on Al_2O_3 is due to the formation of Al-Ga-N ternary compound at the interface [35]. We suspect that in our case the reduction in Al 2p binding energy (71.97 eV) below its metallic level (72.8 eV) could also be due to the formation of Al-Zn-O ternary compound. The distribution of Al atoms in ZnO nanosheets is explained by the quantification data, which were acquired at five different positions on the same sample. All of the regions were maintained with same conditions over the substrate while collecting the data. The obtained Al 2p peak intensities were normalized with respect to the Zn 2p value. There were no significant changes in the observed normalized Al 2p peak intensity, which indicates that the distribution of Al concentration is relatively uniform throughout the sample surface (see S9 supplementary information). The in-depth Al

distribution in ZnO nanosheet matrices is examined by using XPS depth profile measurement. The detailed in –depth Al distribution data was acquired at five different etch times in the ZnO matrices. Significant changes have been observed in the normalized Al 2p peak intensity (see S10 supplementary information), which indicates the non-uniform in-depth distribution of Al concentration in ZnO lattice. It is also found that the ZnO inner layers are pure without any carbon content for 7 min etch time. So, we conclude that the ZnO nanosheets are self-doped with Al element without any impurities.

4. Conclusion

Two dimensional Al doped ZnO nanosheets were grown by low temperature (below 100 °C) solution growth method on Al alloy substrate without using any external seed layer and doping process. The effect of growth temperature on the morphological variations of 2D ZnO nanosheets was studied and it has given an insight about structural morphology, in terms of their thickness and height. The above study revealed that the nanosheets growth starts from 50 °C. The present results also confirmed the in-situ self-doping of ZnO with aluminium in a simplest way. These Al doped ZnO nanosheets are expected to have potential application possibilities in gas sensors, solar cells and energy harvesting devices like nanogenerators. To this aim, future efforts will be devoted to Al doped ZnO nanoheets on various substrates for fabrication of sensors and energy devices.

Acknowledgments

The authors are grateful to the Advanced Facility for Microscopy and Microanalysis (AFMM) for providing the microscopy facility, Indian Institute of Science (IISc), Bangalore. The authors are grateful to the Centre for Nano Science and Engineering (CeNSE) for providing the FESEM facility, Indian Institute of Science (IISc), Bangalore. The authors are grateful to the IPC department for providing XRD facility, Indian Institute of Science (IISc).

References

[1]. Kumar B and Kim S W, Nano energy, 2012, 1(3), 342-355.

[2]. Xu S and Wang Z L, Nano Research, 2011, 4 (11), 1013-1098.

[3].Wang Z L, Applied Physics A, 2007, 88(1), 7-15.

[4]. Wang X, Song J and Wang Z L, J. Mater. Chem, 2007, 17(8), 711-720.

[5]. Wang Z L, J. Phys.: Condens.Matter, 2004, 6 (25), R829–R858.

[6]. Barreca D, Bekermann D, Devi A, Fischer R A, Gasparotto A, Maccato C, Tondello E, Rossi M, Orlanducci S and Terranova M L, Chem. Phys. Lett., 2010, 500 (4), 287-290.

[7]. Bekermann D, Gasparotto A, Barreca D, Devi A, Fischer R A, Kete M, Stangar U L, Lebedev O I, Maccato C, Tondello E, and Tendeloo G V, ChemPhysChem, 2010, 11, 2337 – 2340.

[8]. Gaddam V, Joshi S, Parmar M, Rajanna K and Nayak M M, IEEE Sensors Proc., 2012, 1870-1873.

[9]. Saravanakumar B and Kim S J, J. Phys. Chem. C, 2014, 118, 8831−8836.

[10]. Huang H, Wang H, Li B, Mo X, Long H, Li Y, Zhang H, Carroll D L and Fang G, , Nanotechnology, 2013, 24 (31), 315203.

[11] Barreca D, Ferrucci A P, Gasparotto A, Maccato C, Maragno C and Tondello E, Chem. Vap. Deposition, 2007, 13(11), 618-625.

[12] Barreca D, Gasparotto A, Maccato C, Tondello E, Štangar U L and Patil S R, Surf. Coat. Technol., 2009, 203(14), 2041-2045.

[13]. Wang T, Liu Y, Li G, Sun Z, Lu J, Liu B and Wu M, CrystEngComm, 2011, 13(7), 2661-2666.

[14]. Kim K H, Kumar B, Lee K Y, Park H K, Lee J H, Lee H H, Jun H, Lee D and Kim S W, Scientific Reports 3, 2013,1-6.

[15]. Gupta M K, Lee J H, Lee K Y, and Kim S W, ACS NANO, 2013, 7(10), 8932–8939.

[16]. Sahoo S, Barik S K, Gaur A P S, Correa M, Singh G, Katiyar R. K, Puli V S, Liriano J, and Katiyar R S, ECS J. Solid State Sci. Technol., 2012, 1(6), Q140-Q143.

[17]. Cheng J P, Zhang X B and Luo Z Q, Surf. Coat. Technol., 2008, 202 (19), 4681–4686.

[18]. Cheng J P, Liao Z M, Shi D, Liu F and Zhang X B, J. Alloys Compd., 2009, 480 (2), 741–746.

[19]. Umar A and Hahn Y B, Nanotechnology, 2006, 17(9), 2174–2180.

[20]. Li X, Liang P, Wang L, Yu F, Front. Optoelectron, 2014, 1-4.

[21]. Park J H, Choi H J, Choi Y J, Sohn S H and Park J G, J. Mater.Chem., 2004,14 (1), 35-36.

[22]. Luo H, Xiong G, Yang Z, Li Q, Ma C, Li D, Guo R and Wan Y, Surf. Coat. Technol. (2014).

[23]. Liu B, Xu J, Ran S, Wang Z, Chen D and Shen G, CrystEngComm, 2012, 14(14), 4582-4588.

[24]. Ma M, Tu J P, Yuan Y F, Wang X L, Li K F, Mao F and Zeng Z Y J, Power Sources, 2008, 179(1), 395-400.

[25]. Chin K C, Poh C K, Chong G L, Lin J, Sow C H and Wee A T S, Appl. Phy. A, 2008, 90(4), 623-627.

[26]. Lin C Y, Lai Y H, Chen H W, Chen J G, Kung C W, Vittal R and Ho K C, Energy Environ. Sci., 2011, 4(9), 3448-3455.

[27]. Alkahlout A, Al Dahoudi N, Grobelsek I, Jilavi M and de Oliveira P W, Journal of Materials, 2014, 2014.

[28]. Liang Y C, Ceram. Int., 2012, 38(1), 119-124.

[29]. Sun H, Luo M, Weng W, Cheng K, Du P, Shen G and Han G, Nanotechnology, 2008, 19(12), 125603.

[30]. Guo X, Zhang F, Evans D G and Duan X, Chem. Commun, 2010, 46 (29), 5197-5210.

[31]. Al-Gaashani R, Radiman S, Daud A R, Tabet N and Al-Douri Y, Ceram. Int., 2013, 39(3), 2283-2292.

[32]. Barreca D, Gasparotto A, Maccato C, Maragno C and Tondello E, Surf. Sci. Spectra, 2007, 14(1), 19-26.

[33]. Bai S, Guo T, Zhao Y, Luo R, Li D, Chen A and Liu C C, J. Mater. Chem. A, 1(37), 2013, 11335-11342.

[34]. Dhara S, Imakita K, Giri P K, Mizuhata M and Fujii M, J. Appl. Phy., 2013, 114(13), 134307.

[35]. Sumiya M, Ogusu N, Yotsuda Y, Itoh M, Fuke S, Nakamura T, Mochizuki S, Sano T, Kamiyama S, Amano H and Akasaki I, J. Appl. Phy., 2003, 93(2), 1311-1319.